ARTICLE NO. 79-7047R

J80-173

# Experimental Investigations on Effectiveness, Heat Transfer Coefficient, and Turbulence of Film Cooling

20003
20007

Shao-Yen Ko* and Deng-Ying Liu†
*Chinese Academy of Sciences, Peking, China*

**Experimental studies on the film cooling effectiveness of turbulent flow over an adiabatic flat plate have been carried out. Schlieren photographs for different flow rates are given. Experimental studies of the heat transfer coefficient of an electrically heated flat plate are compared with theoretical results. The fluctuating velocity and turbulence intensity distributions at different sections of the nonisothermal film cooling flowfield were measured by a hot film anemometer. The film cooling effectiveness equations can be modified by the turbulence mixing coefficient.**

## Nomenclature

| | |
|---|---|
| $C_0$ | = turbulence mixing coefficient of the experimental equipment |
| $C_m$ | = turbulence mixing coefficient of the actual turbine engine |
| $h$ | = coefficients of heat transfer by film cooling |
| $M$ | = flow rate, $\rho_s U_s / \rho_\infty U_\infty$ |
| $m$ | = velocity ratio, $U_s/U_\infty$ |
| $Nu_s$ | = Nusselt number, $hx/k_s$ |
| $\dot{q}''$ | = heat flux |
| $Re_s, Re_x$ | = Reynolds number |
| $St$ | = Stanton number |
| $s$ | = slot height |
| $t_{aw}$ | = adiabatic wall temperature |
| $t_\infty, t_s$ | = temperatures of mainstream and film jet |
| $U_\infty, U_s$ | = velocities of mainstream and film jet |
| $x$ | = distance downstream |
| $\beta$ | = turbulence correction factor |
| $\epsilon$ | = turbulence intensity |
| $\eta$ | = effectiveness |

*Subscripts*

| | |
|---|---|
| $aw$ | = adiabatic wall |
| $s$ | = film slot |
| $\infty$ | = freestream conditions |

## Introduction

FILM cooling is widely used in the protective cooling designs of flame tubes, turbine blades, rocket nozzles, and afterburners. The cooling air wall jet entering the hot gas stream effectively thickens the boundary layer, resulting in a change of heat transfer rate.

The adverse effect of film cooling air, especially in the primary combustion region, is to chill the combustion process and thereby reduce combustion efficiency. There is growing awareness of pollutant emissions caused by low combustion efficiency of jet engines, highlighting the need to minimize the effects of the film cooling air. In order to develop a better understanding of the heat transfer characteristics of the film cooling process, the authors made detailed studies of film cooling effectiveness, heat transfer coefficient, and turbulence intensity distributions. The Schlieren pictures reported herein were found to be helpful in understanding the film cooling process.

The turbulence intensity distributions for both the mainstream and the wall jet greatly influence film cooling effectiveness. The so-called "dirty slot" of the actual structures of the film cooling holes in the flame tube has much higher turbulence intensity and much lower effectiveness.

Due to limitations in the capacities of experimental equipment as reported by different authors,[1-3] usually the flow rates $M$ are limited to lower values, while the length of the test plate is long. These two features are contradictory to general practice in the film cooling design of flame tubes. In order to obtain more accurate equations for practical design purposes, special film cooling testing equipment has been constructed. In this equipment, the mainstream is heated by an 130 kW electrical heater to simulate the actual heat flow direction on the film cooled plate. The flow rate $M$ can be varied widely from 0.193 to 3.2. The wall jet of the film cooling process can be divided into three sections as shown in Fig. 1, namely, the initial and main sections and the boundary layer flow. For film cooling design purposes, the main interest is concentrated on the near slot of the initial and main sections.

## Basic Equations of Film Cooling

The velocity and temperature distributions of the mixing region of the flowfield are[4]:

$$\frac{U_\infty - U}{U_\infty - U_\delta} = \left[1 - \left(\frac{y-\delta}{y_1 - \delta}\right)^{3/2}\right]^2 \tag{1}$$

$$\frac{t - t_{aw}}{t_\infty - t_{aw}} = \left[1 - \left(\frac{y_1 - y}{y_1}\right)^3\right]^2 \tag{2}$$

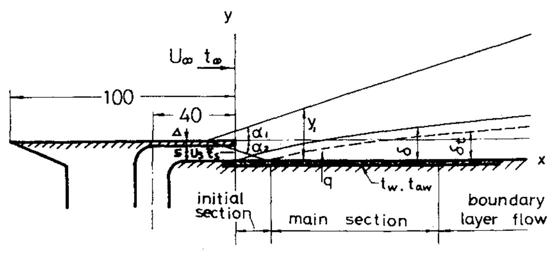


**Fig. 1 Turbulent film cooling over flat plate.**

Presented as Paper 79-7047 at the 4th International Symposium on Air Breathing Engines, Orlando, Fla., April 1-6, 1979; submitted July 2, 1979; revision received Dec. 26, 1979. 

Index categories: Boundary Layers and Convective Heat Transfer—Turbulent; Jets, Wakes, and Viscid-Inviscid Flow Interactions.

*Professor, Head, Division of Heat Transfer, Institute of Engineering Thermophysics. Associate Fellow AIAA.

†Research Associate, Division of Heat Transfer, Institute of Engineering Thermophysics.

Film cooling effectiveness $\eta$ is defined as:

$$\eta = \frac{t_\infty - t_{aw}}{t_\infty - t_s} \tag{3}$$

If the mainstream velocity is very high, the Mach number and the recovery factor $R$ should be considered. Thus, the effectiveness and Stanton number can be written as:

$$\eta = \frac{\left(t_\infty + \frac{R}{2}\frac{U_\infty^2}{c_{p\infty}}\right) - t_{aw}}{(t_\infty - t_s) - \frac{R}{2c_{p\infty}}(U_\infty^2 - U_s^2)} \tag{4}$$

$$St = \dot{q}'' / \left[\left\{c_{p\infty}(t_0 - t_w) + \frac{R}{2}U_\infty^2\right\}\rho_\infty U_\infty\right] \tag{5}$$

Librizzi and Cresci[5] and Stollery and El'Ehwany,[6] proposed a turbulent boundary layer film cooling model to evaluate the effectiveness. The shortcoming of their model is that it is accurate only for very low flow rates and a simple turbulent boundary layer thickness is used. Another interesting heat sink model was introduced by Tribus and Klein.[7] The shortcoming is its limitation to low flow rates and to only the far side of the film slot region.

## Experimental Equipment

For the adiabatic wall temperature measurements, the test plate is made of stainless steel with a thickness of 12 mm. There are 40 deep grooves 11.5 mm deep at the back side of the test plate along the flow direction to eliminate heat conduction loss.

A 0.5-mm-thick nickel-chromium band is used for the heat transfer coefficient test as well as Schlieren photographic equipment with a light beam diameter of 80 mm and a DISA-type 55-m hot film anemometer and 55R33 hot film probe.

## Flowfield Measurements

Figure 2 is the measured dimensionless velocity distribution of film cooling which is in agreement with Eq. (1). The measured dimensionless temperature distribution is given in Fig. 3.

## Schlieren Photographs

Figure 4 shows some Schlieren pictures of the film cooling process with both sharp edge and square edge slot plates. The major heat transfer data are obtained with the insertion of the square edge slot plate. The sharp edge slot plate is used for Schlieren photographs and boundary layer formation studies.

## Film Cooling Effectiveness

The large amounts of experimental data given by the present authors as shown in Fig. 5 cover a much wider range of flow rates. It is interesting to note the difference between the regions of $M<1$ and $M>1$. At the near slot region, say $x/s<44.5$, after $M$ reached a certain value, $\eta$ is no longer increasing. This means that the cooling effect is no longer increasing beyond that range even though the flim coolant is increased. From Fig. 5, the following film cooling effectiveness equations can be obtained:

1) For $M = \rho_s U_s / \rho_\infty U_\infty < 1$:

$$\eta = 2.73\, M^{0.4} (x/s)^{-0.38}, \quad x/s \leq 20 \tag{6}$$

$$\eta = 5.44\, M^{0.4} (x/s)^{-0.58}, \quad 20 \leq x/s < 150 \tag{7}$$

$$\eta = 2.04 (x/s)^{-0.38} \tag{8}$$

In the region $x/s<65.2$ and $0.45<M<1$, the lower value of $\eta$ from the last two equations is chosen.

2) For $1 \leq M < 2$:

$$\eta = 1.96\, M^{0.55} (x/s)^{-0.38}, \quad x/s < 150 \tag{9}$$

3) For $2 \leq M < 3.5$:

$$\eta = 2.71 (x/s)^{-0.38}, \quad x/s < 150 \tag{10}$$

Based upon the same experimental data, the above equations can be simplified to Eqs. (11) and (12) for design purposes.

4) For $M = 1 \sim 1.5$:

$$\eta = (0.1 \cdot x/Ms)^{-0.5}, \quad 5 < x/Ms < 150 \tag{11}$$

5) For $M = 1.75 \sim 3.19$:

$$\eta = 1.75 (x/Ms)^{-0.35}, \quad 5 < x/Ms < 100 \tag{12}$$

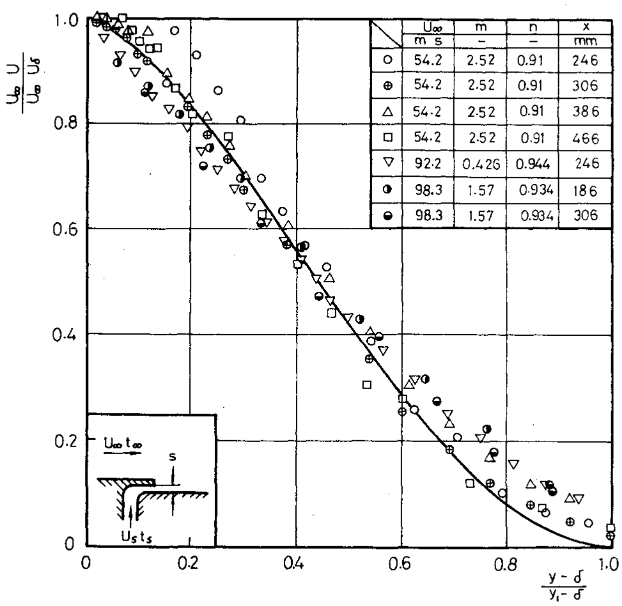


**Fig. 2 Dimensionless velocity distribution of film cooling.**

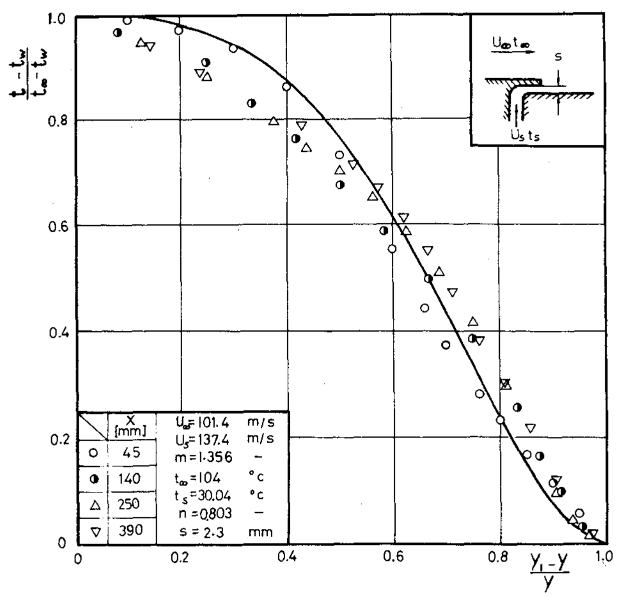


**Fig. 3 Temperature distribution of film cooling over adiabatic flat plate.**

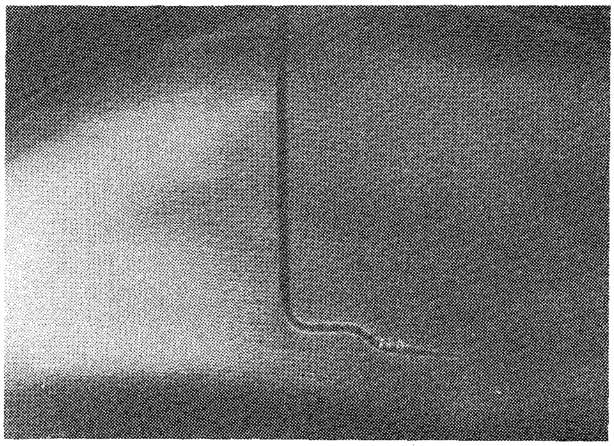

a) $U_\infty = 71.1$ m/s, $U_s = 37.9$ m/s, $t_\infty = 54.3$°C, $t_s = 34.7$°C, $M = 0.83$.

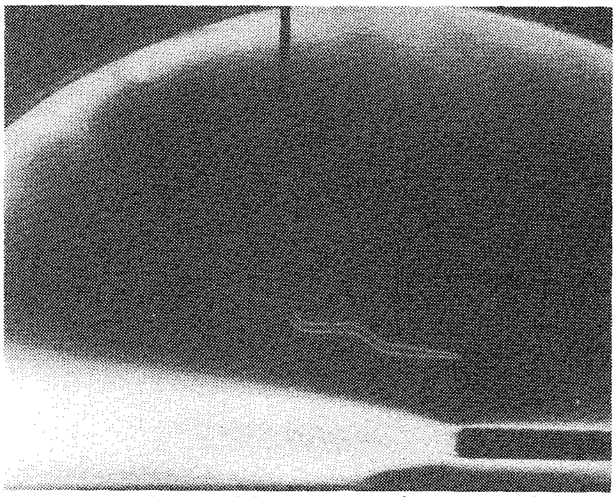

b) $U_\infty = 71.1$ m/s, $U_s = 62.0$ m/s, $t_\infty = 54.5$°C, $t_s = 33.3$°C, $M = 0.95$.

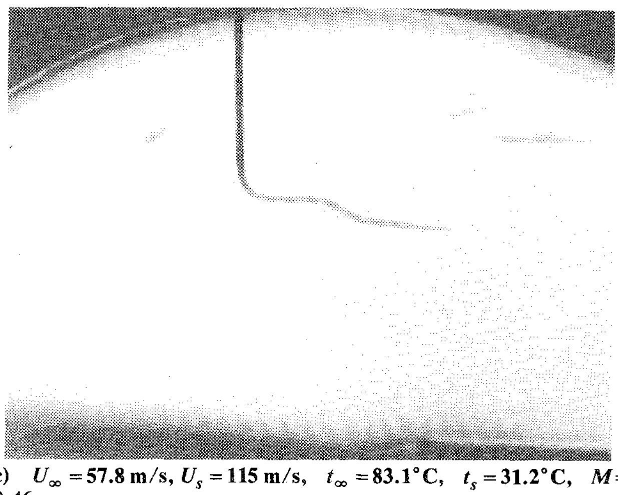

c) $U_\infty = 57.8$ m/s, $U_s = 115$ m/s, $t_\infty = 83.1$°C, $t_s = 31.2$°C, $M = 2.46$.

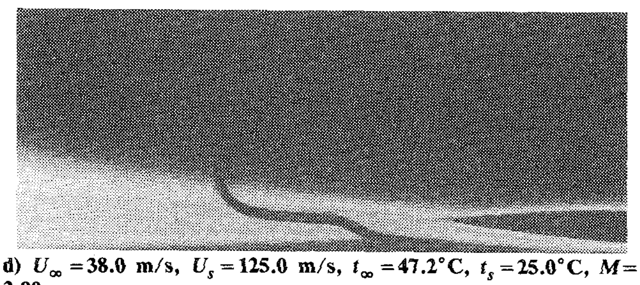

d) $U_\infty = 38.0$ m/s, $U_s = 125.0$ m/s, $t_\infty = 47.2$°C, $t_s = 25.0$°C, $M = 3.80$.

**Fig. 4 Schlieren photographs.**

Figure 6 compares the effectiveness correlations by the present authors and others[1,8,9] for $M = 0.3$, 0.8, 1.3, and 1.5, and $x/s$ chosen between 10-100. Figures 7 and 8 compare the present effectiveness correlations with different authors[16,18] and actual turbines.

## Coefficient of Heat Transfer in Film Cooling

For design purposes, the heat flow rate by film cooling over the high temperature wall must be evaluated. In the calculation of heat flow rate, the actual value of the coefficient of heat transfer and the proper temperature difference[10] must be known. The heat flux can be evaluated by the following equation:

$$q = h(t_{aw} - t_w) \tag{13}$$

Some recent experimental results[11-13,18] and theoretical evaluations[14,15] demonstrate that the coefficient of heat transfer by film cooling is quite different from that of conventional forced convection, particularly at low flow rates and at the near slot region.

## Turbulence Mixing Coefficient

Recently, turbine engines designers have been interested in the reduction of turbulence in gas streams in order to improve engine performance and film cooling stability. As pointed out by Juhasz-Marek,[16] the effectiveness of film cooling is strongly influenced by the turbulence mixing coefficient $C_0$, as shown in the following equation:

$$\eta = \frac{1}{1 + C_0(x/Ms)} \tag{14}$$

where the turbulence mixing coefficient $C_0$ is the mean value of initial intensities for main stream $\epsilon_f$ and jet flow $\epsilon_s$. At present, the following equation is suggested for the evaluation of the turbulence mixing coefficient:

$$C_0 = \epsilon_f + 0.4(|\epsilon_s - \epsilon_f|) \tag{15}$$

## Comparison of Experimental and Calculated Results

Spalding[15] evaluated the coefficient of heat transfer by film cooling in the turbulent flow by the Patankar-Spalding method.[14] Figure 9 compares the Stanton number results calculated by Spalding[15] and the experimental results of the present authors. It is interesting to note that the tendency of a gradual increase in the coefficient of heat transfer by film cooling is confirmed by the work of Spalding in the near slot region. For a given value of Stanton number, the calculated result gives a higher value of $x/s$ than the experiment. The possible explanation for this discrepancy is that the actual external boundary layer of the flowfield as measured by the present authors is much wider than the theoretical value, and the actual external boundary is gradually diminished downstream. This trend can be observed in the Schlieren pictures.

## Correlations of Coefficients of Heat Transfer by Film Cooling

The experimental results of coefficient of heat transfer by film cooling can be correlated in two ranges, namely, $M \le 1$ and $1 < M < 2$.

For the $M \le 1$ and $8 \le x/s < 60$ range, the following correlation can be obtained from Fig. 10:

$$Nu_g = 0.144\, Re_g^{0.66} M^{-0.1} \tag{16}$$

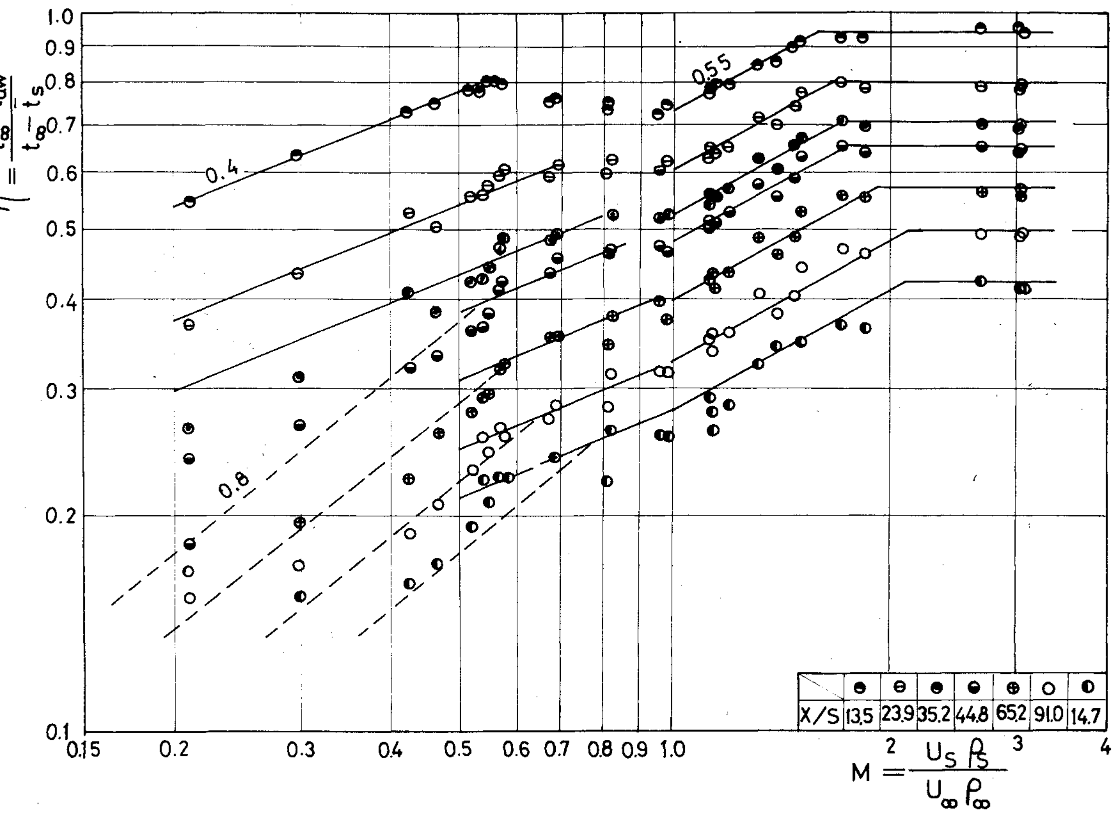


**Fig. 5 Variations of effectiveness with respect to flow rate $M$.**

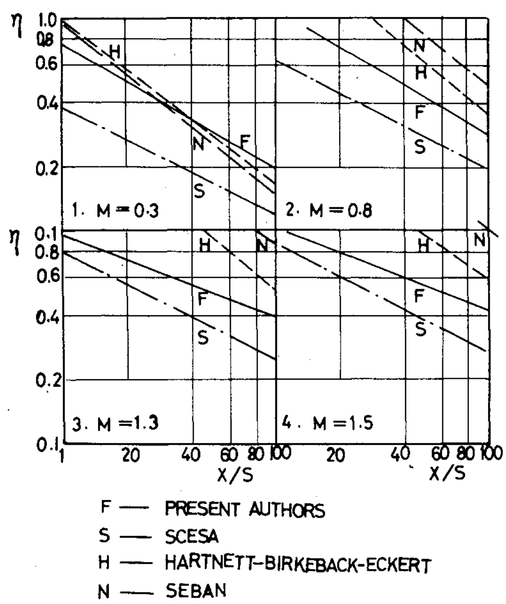


**Fig. 6 Comparisons of present effectiveness correlations with different authors.**

where

$$Nu_g = hx/k_g$$

$$Re_g = U_g x/\nu_g$$

For the $1<M<2$ range and higher flow rates, the film jet Reynolds number $Re_x$ has a stronger influence on heat transfer coefficient near the slot region.

Figures 11-13 show that $Nu_s$ is increasing as $Re_x$ increases. These results can be expressed in the following equations:

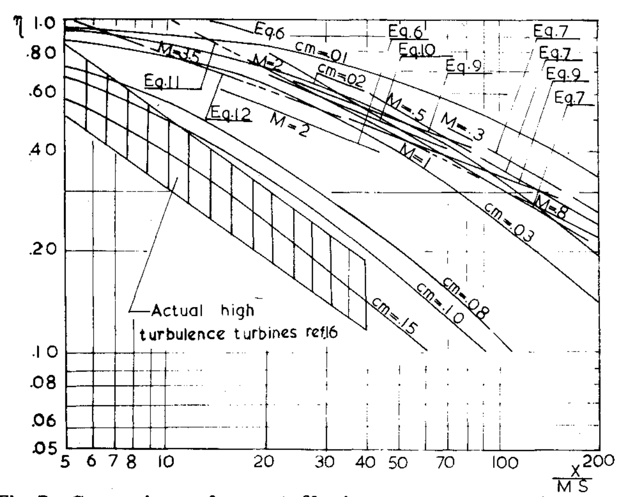


**Fig. 7 Comparisons of present effectiveness correlations with respect to actual turbines.**

For $1<M<2$ and $x/s<10$:

$$Nu_s = 0.057\, Re_x^{0.7} \tag{17}$$

where $Re_x = U_s x/\nu_s$.

For $1<M<2$ and $10 \leq x/s \leq 35$:

$$Nu_s = 6.39 \cdot 10^{-5} (Re_x/M)^{1.3} \tag{18}$$

Equation (17) is compared in Fig. 14 with the results given by several authors, such as Seban and Back[12] for $0.5<M<1.3$:

$$Nu_x = 0.069 (Re_x x/s)^{0.7} \tag{19}$$

and Myers et al.[13] for $M<1.3$, $x/s<50$ for $\phi = \epsilon_H/\epsilon_M = 2$:

$$Nu_x = 0.10 Re_s^{0.8} (x/s)^{0.44} \tag{20}$$

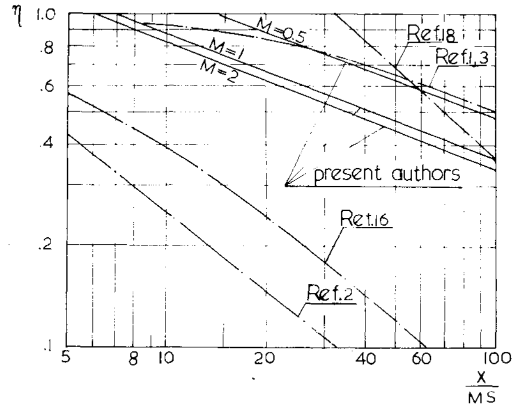


Fig. 8 Variations of effectiveness with respect to $x/Ms$ by different authors.

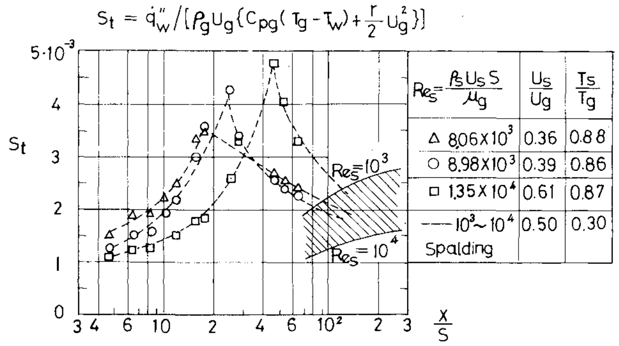


Fig. 9 Comparison of experimental results of local Stanton number with theoretical results of Spalding.

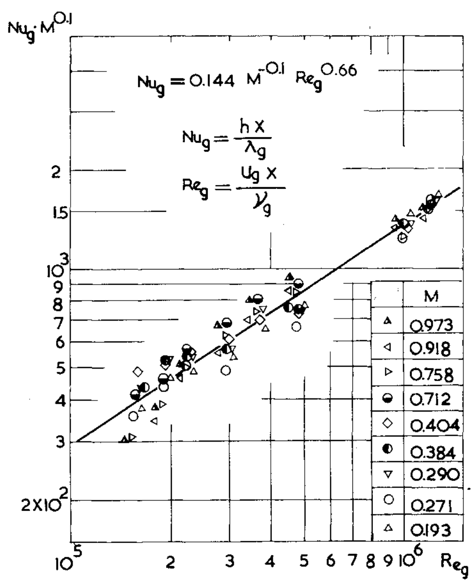


Fig. 10 Coefficients of heat transfer over flat plate by film cooling for $8 \leq x/s \leq 60$ and $M \leq 1$.

## Calibration of Hot Film Anemometer for Nonisothermal Flowfield

It is difficult to calibrate the hot film anemometer for a nonisothermal flowfield[17] such as in the film cooling process. Normally the anemometer is calibrated in the wind tunnel at room temperature. If the temperature of the flowfield under investigation is nonisothermal and different from room temperature, special effort must be made for such calibration. Generally speaking, there are two modification methods, temperature calibration or automatic circuit compensation.

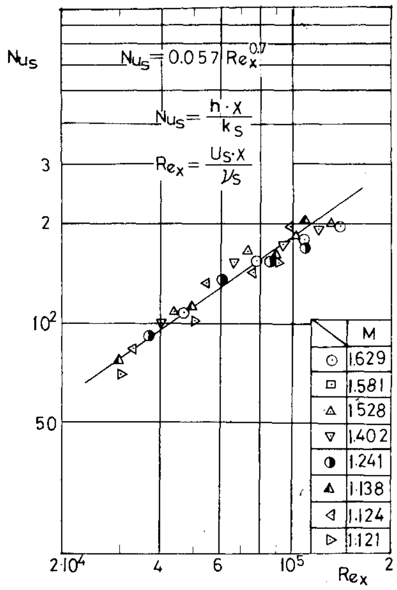


Fig. 11 Coefficients of heat transfer over flat plate by film cooling for $x/s < 10$ and $1 < M < 2$.

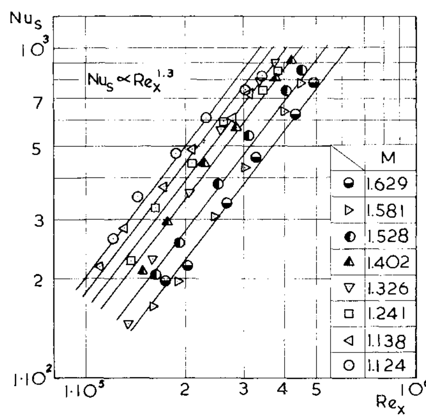


Fig. 12 Variations of $Nu_s$ with respect to $Re_x$ for $10 \leq x/s \leq 35$ and $1 < M < 2$.

The temperature calibration method is used now with some improvements. During the calibration process two improvements are introduced. The first is the introduction of a calibration curve of bridge voltage $V$ and Peclet number instead of the normal voltage-velocity curve. Thus the similarity of heat convection of hot film sensor is maintained if the Peclet number of the test point is equal to the Peclet number of the calibration wind tunnel. If the temperature of the test point is $t$ and the calibration temperature is 10° C, then,

$$Pe_t = Pe_{10} \tag{21}$$

or

$$U_t = U_{10}(\nu_t/Pr_t)/(\nu_{10}/Pr_{10}) \tag{22}$$

where $U_{10}$ is the velocity of the calibration wind tunnel at room temperature. During the calibration, the room temperature was 10°C.

The second improvement is the introduction of the static calibration of the resistance-temperature curve at zero velocity. Once the stream temperature of the given test point is known, the proper stream velocity can be evaluated from the $V$-$Pe$ curve and the resistance-temperature curve.

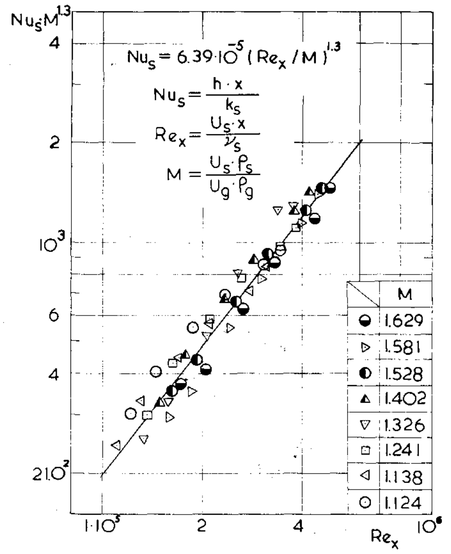


**Fig. 13 Coefficients of heat transfer over flat plate by film cooling for $10 \leq x/s \leq 35$ and $1 < M < 2$.**

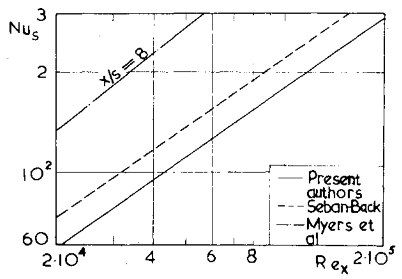


**Fig. 14 Comparison of $Nu_s$ correlations by present authors and those by Seban and Myers.**

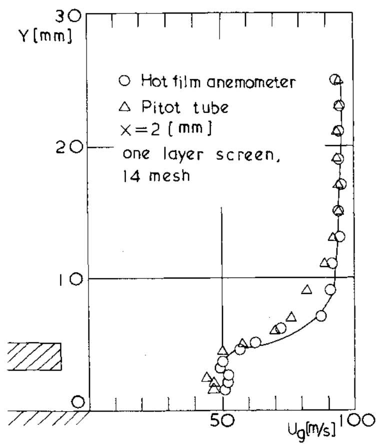


**Fig. 15 Comparison of velocity profile of film cooling measured by hot film anemometer and Pitot tube.**

## Velocity and Turbulence Distributions Measured by Hot Film Anemometer

Figure 15 compares the velocity profile of film cooling measured by a hot film anemometer and a Pitot tube. After the proper calibrations mentioned above, the agreement is good. The distributions for velocity, instantaneous velocity, and turbulence intensity as measured by hot film anemometer are given in Fig. 16. The turbulence intensity distributions at different sections and different jet velocities are given in Fig. 17.

From such experimental results, the characteristic initial turbulence intensities for both the mainstream and the film jet

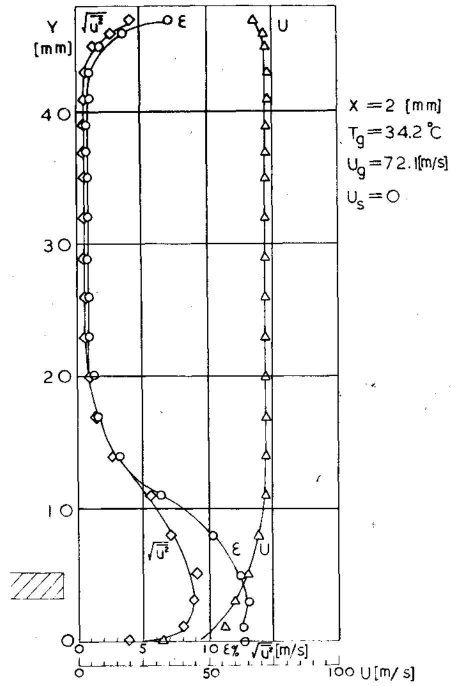


**Fig. 16 Velocity, instantaneous velocity, and turbulence intensity distributions measured by hot film anemometer.**

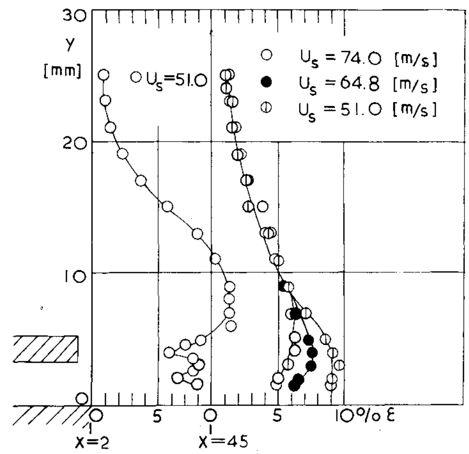


**Fig. 17 Turbulence intensity distributions at different sections and jet velocities.**

can be chosen as follows:

$$\text{For the mainstream:} \quad \epsilon_f = 2\% \tag{23}$$

$$\text{For the film jet:} \quad \epsilon_s = 10\% \tag{24}$$

Thus from Eq. (15), the turbulence mixing coefficient $C_0$ is:

$$C_0 = 5\% \tag{25}$$

## Turbulence Correction Factor for Effectiveness

In the actual calculation of the wall temperatures of the film cooled parts, the turbulence correction factor $\beta$ for effectiveness is suggested as follows:

$$\eta_{\text{turb}} = \beta \eta \tag{26}$$

where $\beta$ is defined as:

$$\beta = \frac{1 + C_0 (x/Ms)}{1 + C_m (x/Ms)} \tag{27}$$

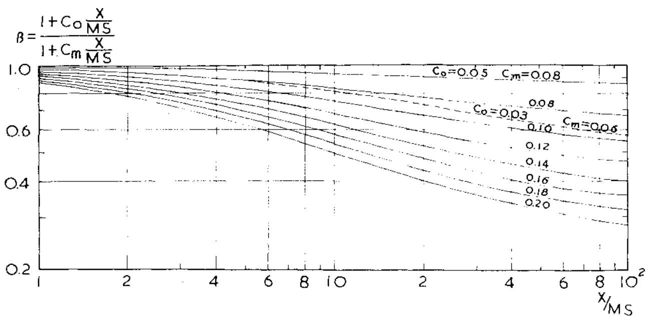


**Fig. 18 Variations of turbulence mixing coefficients $C_0$ and $C_m$ with respect to $x/Ms$.**

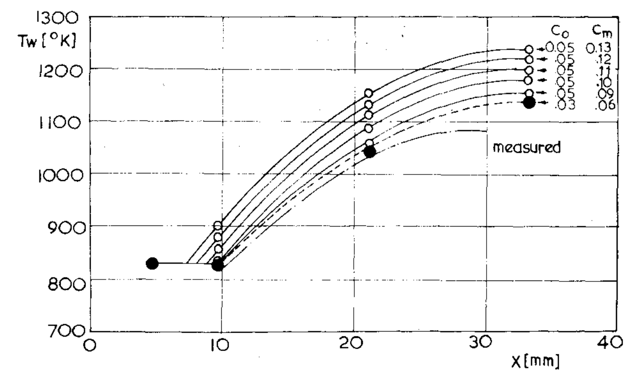


**Fig. 19 Calculated results of temperature distribution of film cooled flame tube.**

The value $\beta$ represents the turbulence correction of $\eta$ not only by the experimental equipment turbulence mixing coefficient $C_0$, but also by the turbulence mixing coefficient of the actual turbine engine $C_m$. The actual values of $C_m$ for turbine engines can vary 10-15%. These results have been used in the authors' computer program of the temperature and heat load calculations for film cooled walls. It is obvious that the lower the turbulence intensity of gas stream inside the turbine, the higher the film cooling efffectiveness achieved.

Figure 18 shows the variations of turbulence mixing coefficients $C_0$ and $C_m$ with respect to $x/Ms$. It is obvious that the lower the turbulence intensity of the gas stream inside the turbine engine, the higher the film cooling effectiveness achieved.

As an example, Fig. 19 shows the calculated wall temperature of the film cooled flame tube of a typical aircraft gas turbine. In this calculation, the equations of effectiveness, heat transfer coefficient, and turbulence mixing coefficient presented herein are all used.

## Conclusions

1) The velocity and temperature distributions are obtained for film cooling process.

2) Experimental correlations of effectiveness and coefficients of heat transfer for film cooling are presented.

3) The experimental data on the turbulence distributions for nonisothermal film cooling process are obtained.

4) The equations for effectiveness, heat transfer coefficient, and turbulence mixing coefficient will be useful in the evaluation of heat transfer characteristics of film cooled engine parts.

## References


[1] Hartnett, J. P., Birkeback, R. C., and Eckert, E.R.G., "Velocity Distributions, Temperature Distributions, Effectiveness and Heat Transfer for Air Injection through a Tangential Slot into a Turbulent Boundary Layer," *Journal of Heat Transfer, Transactions of ASME*, Vol. 83, 1961, p. 293.

[2] Nishiwaki, N., Hirata, M., and Tsuchida, A., "Heat Transfer on a Surface Covered by Cold Air Film," *International Developments in Heat Transfer*, Pt. IV, 1961.

[3] Hartnett, J. P., Birkeback, R. C., and Eckert, E.R.G., "Velocity Distributions, Temperature Distributions, Effectiveness and Heat Transfer in Cooling of a Surface with a Pressure Gradient," *International Developments in Heat Transfer*, Pt. IV, 1961.

[4] Schlichting, H., *Boundary Layer Theory*, translated by J. Kestin, McGraw-Hill Book Co., Inc., New York, 1955, p. 492.

[5] Librizzi, J., and Cresci, R. J., "Transpiration Cooling of a Turbulent Boundary Layer in an Axisymmetric Nozzle," *AIAA Journal*, Vol. 2, 1964, p. 617.

[6] Stollery, J. L. and El'Ehwany, A.A.M., "On the Use of a Boundary Layer Model for Correlating Film Cooling Data," *International Journal of Heat Mass Transfer*, Vol. 10, 1967, p. 101.

[7] Tribus, M. and Klein, J., "Forced Convection from Nonisothermal Surfaces," *1952 Heat Transfer Symposium*, University of Michigan, Ann Arbor, 1953, p. 211.

[8] Scesa, S., "Effect on Local Normal Injection on Flat-Plate Heat Transfer," Ph.D. Thesis, University of California, Berkeley, 1954.

[9] Seban, R. A., "Heat Transfer and Effectiveness for a Turbulent Boundary Layer with Tangential Fluid Injection," *Journal of Heat Transfer, Transactions of ASME*, Vol. 82, 1960, p. 303.

[10] Eckert, E.R.G., "Transpiration and Film Cooling," *Heat Transfer Symposium*, University of Michigan, Ann Arbor, 1953, p. 195.

[11] Eriksen, V. L., "Film Cooling Effectiveness and Heat Transfer with Injection through Holes," NASA CR-72991, N72-14945, 1971.

[12] Seban, R. A. and Back, L. H., "Effectiveness and Heat Transfer for a Turbulent Boundary with Tangential Injection and Variable Free Stream Velocity," *Journal of Heat Transfer, Transactions of ASME*, Vol. 84, 1962, p. 235.

[13] Myers, G. E., Schauer, J. J., and Eustis, R. H., "Heat Transfer to Plane Turbulent Wall Jets," *Journal of Heat Transfer, Transactions of ASME*, Vol. 85, 1963, p. 209.

[14] Patankar, S. V. and Spalding, D. B., *Heat and Mass Transfer in Boundary Layers*, Morgan-Grampian, London, 1967.

[15] Spalding, D. B., "Boundary Layer Theory Applied to Film-Cooling Processes," *Progress in Heat and Mass Transfer*, Vol. IV, 1971, p. 279.

[16] Juhasz, A. J. and Marek, C. J., "Combustor Liner Film Cooling in the Presence of High Free Stream Turbulence," NASA TN D-6360, 1971.

[17] Pessoni, D. H. and Chao, B. T., "A Simple Technique for Turbulence Measurements in Nonisothermal Air Flows," Paper presented at Interntional Heat Transfer Conference, Tokyo, Vol. 278, 1974.

[18] Goldstein, R. J., Shavit, G., and Chen, T. S., "Film Cooling Effectiveness with Injection Through a Porous Section," *Journal of Heat Transfer, Transactions of ASME*, Vol. 87, 1965.